Available online at www.CivileJournal.org

Civil Engineering Journal

(E-ISSN: 2476-3055; ISSN: 2676-6957)

Vol. 11, No. 03, March, 2025

Mechanical Properties of Sustainable Base Course Binder Incorporating GGBFS and Spent FCC Catalyst

Sajjad E. Rasheed [1], Waqed H. Hassan [2], Mohammed Y. Fattah [3*]

[1] *Civil Engineering Department, University of Karbala, Karbala 56001, Iraq.*

[2] *College of Engineering, University of Warith Al-Anbiyaa, Kerbala 56001, Iraq.*

[3] *Civil Engineering Department, University of Technology, Baghdad 10056, Iraq.*

Received 10 November 2024; Revised 16 January 2025; Accepted 04 February 2025; Published 01 March 2025

Abstract

This study investigates the feasibility of utilizing ground granulated blast furnace slag (GGBFS) and spent fluid catalytic cracking (FCC) catalyst as partial cement replacements in pavement base course materials. Various blends of GGBFS and FCC catalyst were evaluated as binders for unbound granular base (UGB) material, with total binder content fixed at 10% by weight. Mechanical properties were assessed through unconfined compressive strength (UCS) and splitting tensile strength tests at 3, 7, 28, and 56 days. Microstructural analysis was conducted using scanning electron microscopy (SEM) and X-ray diffraction (XRD). Results indicate that an optimal blend of 60% FCC and 40% GGBS achieved the highest UCS of 9.6 MPa at 56 days, exceeding typical requirements for cement-treated base materials. All investigated mix proportions surpassed the minimum 28-day strength requirement of 4 MPa for pavement base applications. Splitting tensile strength results corroborated compressive strength trends, with enhanced tensile-to-compressive strength ratios suggesting improved crack resistance potential. Microstructural analysis revealed a dense, well-reacted cementitious system supporting the observed mechanical performance. These findings demonstrate the technical feasibility and potential environmental benefits of incorporating high volumes of GGBS and spent FCC catalyst in pavement base materials, offering a sustainable alternative to conventional cement-based binders.

Keywords: Ground Granulated Blast Furnace Slag (GGBFS); Spent Fluid Catalytic Cracking (FCC) Catalyst; Pavement Base Course; Unconfined Compressive Strength; Splitting Tensile Strength; Microstructural Analysis; Sustainable Construction Materials.

1. Introduction

The use of industrial by-products and waste materials in pavement applications, specifically for base/subbase layers, has become an increasing concern because of environmental issues coupled with the necessity to incorporate sustainable construction practices [1–3]. This strategy tackles waste disposal issues as well and may have economic and environmental advantages [4, 5]. Building on this focus, recent studies have concentrated on identifying and evaluating new sustainable pavement materials. For example, Ramírez-Vargas et al. (2024) [6] reviewed sustainable aggregates derived from solid waste, noting their feasibility as conventional aggregate replacements. Sathvik et al. (2023) [7] investigated geopolymer concrete incorporating alternative materials suitable for pavements, while Ullas & Bindu (2024) [8] examined locally sourced supplementary cementitious materials for stabilized macadam layers.

Among the widely used supplementary cementitious materials is ground granulated blast furnace slag (GGBFS), a by-product of the iron and steel industry. GGBFS exhibits pozzolanic activity [9], making it suitable as a partial replacement for ordinary Portland cement. Research has shown that GGBFS can improve the mechanical properties of

* Corresponding author: 40011@uotechnology.edu.iq

http://dx.doi.org/10.28991/CEJ-2025-011-03-012

soil and concrete mixtures. Gholampour & Ozbakkaloglu (2017) [10] reported that incorporating GGBFS into concrete significantly enhanced strength and durability. Likewise, Ika Putra & Shahin (2019) [11] demonstrated that adding slag improved the performance of expansive soil in road pavement subgrades. Further advancements were noted by Amulya & Ravi Shankar (2020) [12], who observed that substituting normal base courses with stabilized lateritic soil using GGBFS and an alkali solution improved both strength and durability. Similar positive outcomes were reported by Arulrajah et al. (2016) [13] when GGBFS was applied in pavement subbase materials stabilized with recycled construction and demolition waste.

In addition to GGBFS, spent fluid catalytic cracking (FCC) catalyst, an oil refinery by-product, has attracted interest. Its highly aluminous and siliceous nature provides pozzolanic properties [14]. Rodríguez et al. [15] utilized geopolymer synthesis from spent FCC catalyst residue, while Payá et al. (1999) [16] found that this residue, used as a mineral admixture, improved early-strength development in cement pastes. More recently, research has explored applying spent FCC catalyst with asphalt binders. For instance, Xue et al. (2020) [17] studied its interaction with an asphalt binder. Rasheed et al. (2024) [18] investigated a composite binder combining cement bypass dust and spent FCC catalyst, demonstrating possible benefits of blending multiple waste materials in pavement applications.

To quantify the performance of these materials, unconfined compressive strength (UCS) testing is commonly used. The method for determining the UCS of cohesive soil is provided in D1633M-17 [19], which can be utilized for stabilized base course materials. Lim and Zollinger (2003) [20] developed methods to estimate the compressive strength of blended cement-treated aggregate base material, which can be incorporated into mixtures containing GGBFS and spent FCC catalyst. Previous research evaluated industrial by-products for soil stabilization and pavement using UCS tests. For instance, Al-Hdabi et al. (2014) [21] investigated high calcium fly ash for improving cold bitumen emulsion mixtures, while Taha (2020) [22] examined the effect of cement kiln dust on reclaimed asphalt pavement materials, using UCS as a key performance indicator. This highlights the flexibility and value of UCS testing in evaluating new types of pavement materials. Splitting tensile strength testing, conducted in accordance with ASTM C469 [23], can also be employed to assess resistance to cracking under tensile loads. Although this standard is designed for cylindrical concrete specimens, it can be adapted for stabilized base course materials to understand their tensile performance.

Beyond mechanical testing, microstructural analysis provides key information about hydration products and pore structures in cementitious systems. Scanning electron microscopy (SEM) has been used extensively to characterize microstructural features. Chen et al. (2004) [24] employed SEM to study C-S-H gels, while Wolter et al. (2019) [25] examined radionuclide retention in these gels. The ratio of calcium to silica (Ca/Si) in C-S-H gels influences material properties, and SEM allows for its detection. Madadi and Wei (2022) [26] characterized gels with various polymer modifications, and Fan et al. (2023) [27] investigated how the Ca/Si ratio affects alkali-activated ultra-high-performance concrete. Such analysis provides valuable information for optimizing cementitious materials in pavement applications.

A wide range of industrial by-products have been explored for pavement purposes. Mohajerani et al. (2020) [28] reviewed recycling waste rubber tires into construction materials, including pavements. Alemshet et al. (2023) [29] used fly ash and powdered ground steel slag to improve expansive subgrade soil, while Kumar et al. (2023) [30] examined various waste materials as binders for sustainable stabilization. Kedar et al. (2024) [31] applied response surface methodology to optimize industrial waste blends in road construction. Other research, such as [32], studied multi-source solid-waste-based soil stabilization, and Zhang et al. (2021) [33] evaluated cement-stabilized recycled mixtures with recycled concrete aggregate and crushed brick. Recent research explored utilizing waste materials and industrial by-products in pavement applications. Mohajerani et al. (2020) [28] reviewed the recycling of waste rubber tires in construction materials, with a focus on their application within pavement structures. Alemshet et al. (2023) [29] explored means of improving expansive subgrade soil by the application of fly ash and powdered ground steel slag. Kumar et al. (2023) [30] investigated the use of different types of waste materials as binders for sustainable stabilization. Kedar et al. (2024) [31] optimized industrial waste combinations in road construction using response surface methodology.

While previous studies have explored various industrial by-products in pavement applications, limited research exists on the combined use of GGBFS and spent FCC catalyst, particularly regarding their optimal proportions and synergistic effects in base course materials. Understanding the mechanical properties, microstructural characteristics, and long-term strength development of binary blends incorporating these materials is crucial for their practical implementation in sustainable pavement construction. To address this gap, a comprehensive experimental program was designed to evaluate various GGBFS-FCC blends through unconfined compressive strength testing, splitting tensile strength assessment, and detailed microstructural analysis using SEM and XRD techniques. This systematic approach enables the determination of optimal blend ratios while providing insights into the fundamental mechanisms governing strength development in these binary systems.

The aim of this research is to investigate the mechanical properties and microstructural characteristics of base course binders incorporating ground granulated blast furnace slag (GGBFS) and spent fluid catalytic cracking (FCC) catalyst as partial replacements for traditional cement. The objectives are as follows:

- Evaluating the unconfined compressive strength (UCS) of base course mixtures containing various proportions of GGBFS and spent FCC catalyst as partial cement replacements.

- Assessing the splitting tensile strength of the developed mixtures to understand their resistance to cracking under tensile stresses.
- Analyzing the microstructural characteristics of the binders using scanning electron microscopy (SEM) and X-Ray diffraction analysis to understand the formation of hydration products and their influence on mechanical properties.
- Determining the optimal proportion of GGBFS and spent FCC catalyst in the binder that yields the best mechanical properties for base course applications.
- Investigating the potential synergistic effects between GGBFS and spent FCC catalyst in binary blended systems.

2. Materials

2.1. Unbound Granular Base (UGB)

This study utilized a crushed gravel aggregate as the unbound granular base (UGB) material, sourced from local quarries supplying an asphalt pavement plant. The aggregate was processed to comply with Iraqi standard R7 specifications for base course materials [34]. Grain size analysis (Figure 1) revealed a well-graded distribution ranging from 3/2 in. to No. 200 sieves. The composition comprised 55% coarse fraction (>No. 4 sieve), 35% fine fraction (No. 4 to No. 200 sieves), and 10% fines (<No. 200 sieve). This distribution ensures adequate gradation for particle interlock while maintaining stability.

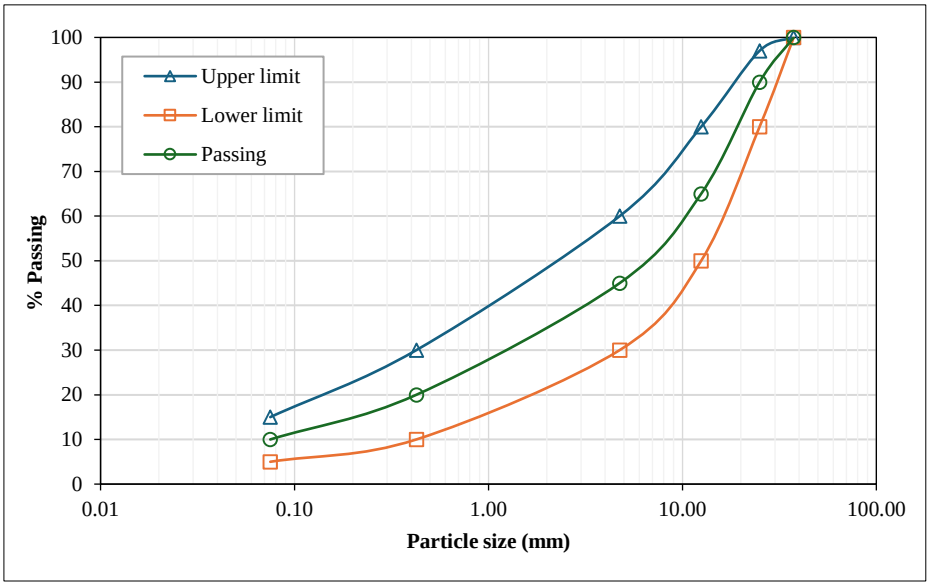

Figure 1. Grain size analysis curve for unbound granular base material

Physical and engineering properties of the UGB material were characterized through various tests. The fine fraction exhibited a liquid limit of 14%. Modified Proctor compaction testing yielded a maximum dry density of 2.39 g/cm³ at 5.4% optimum moisture content. After 4 days of soaking, the California Bearing Ratio (CBR) was 83%. The Los Angeles abrasion test resulted in a 29% loss. The unconfined compressive strength of untreated specimens compacted to 100% modified Proctor density was 580 kPa. All tested properties met or exceeded the requirements set forth in Iraqi standard R7-2003 for base course aggregate materials, as summarized in Table 1. These results indicate the suitability of the selected UGB material for its intended application in pavement construction.

Table 1. Properties of UGB

Test	Result	Requirements	Test Standard
SO_3 content (%)	1.14%	< 5%	ASTM C1580 [35]
TSS content (%)	2.12%	< 5%	ASTM C1580 [35]
Gypsum content (%)	2.3%	< 5%	ASTM D 2974 [36]
Liquid limit (%)	14	< 25%	ASTM D 4318-10 [37]
Plasticity Index (%)	-	< 4%	ASTM D 4318-10 [37]
California Bearing Ratio (%)	83%	>80%	ASTM C131 [38]
L.A. abrasion loss (%)	32.10%	< 45%	ASTM C 131-14 [39]
MDD (g/cm³)	23.9 kN/m³	-	ASTM D 1557 [40]

2.2. GGBFS

Ground granulated blast furnace slag (GGBFS) was sourced from a local supplier in Baghdad, Iraq. X-ray fluorescence (XRF) and X-ray diffraction (XRD) analyses were conducted to characterize its chemical composition and crystalline structure, respectively. XRF analysis shown in Table 2 revealed the predominant oxides in GGBFS as CaO (58.5%), SiO_2 (15.7%), and Al_2O_3 (13.2%), collectively constituting 87.4% of the total composition. Additional components include MgO (8.4%), SO_3 (1.8%), and K_2O (0.4%), with the remaining 2% attributed to trace elements.

Table 2. Chemical compositions of GGBFS

Oxide	Content (%)
CaO	58.5
SiO_2	15.7
Al_2O_3	13.2
MgO	8.4
SO_3	1.8
K_2O	0.4
Others	2

XRD analysis presented in Figure 2 exhibited a broad hump between 20° and 35° 2θ, indicative of an amorphous glassy phase characteristic of GGBFS. Minor crystalline peaks observed around 29° and 32° 2θ suggest the presence of trace crystalline phases, potentially gehlenite or akermanite. The predominantly glassy nature of the GGBFS is favorable for its reactivity in cementitious systems. The chemical composition and amorphous structure of the GGBFS indicate its potential efficacy as a supplementary cementitious material.

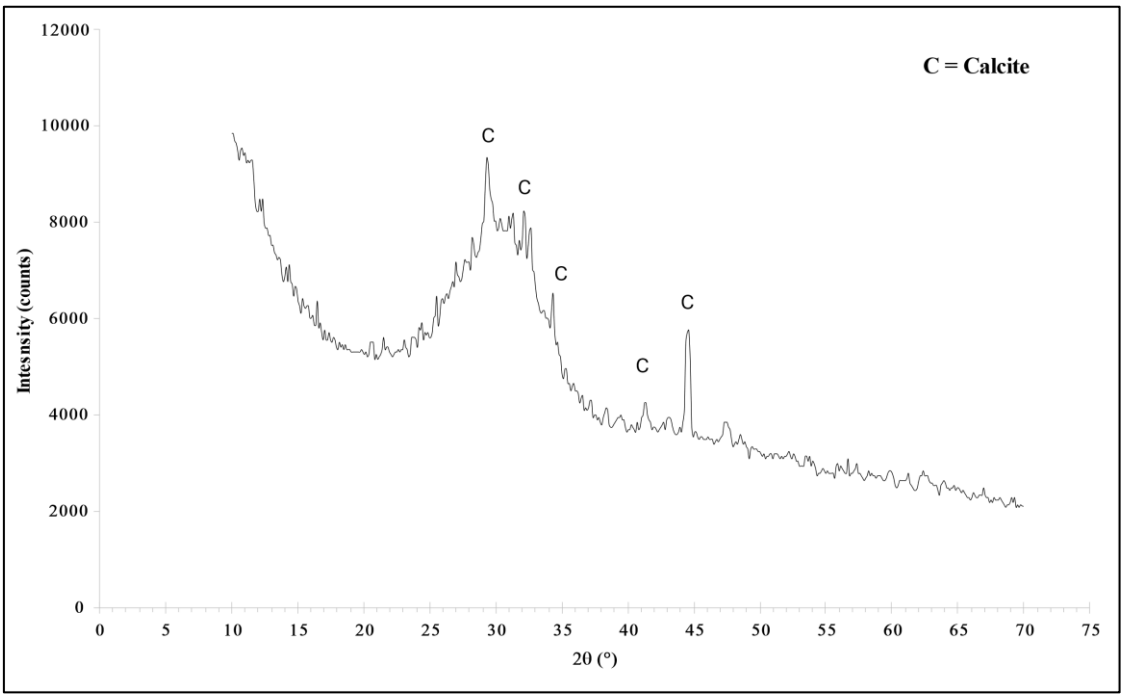

Figure 2. XRD data of GGBFS

2.3. Spent FCC Catalyst

The spent fluid catalytic cracking (FCC) catalyst, sourced from the oil refinery in Karbala city, was characterized using both X-ray fluorescence (XRF) spectroscopy and X-ray diffraction (XRD) analysis.

XRF analysis, as shown in Table 3, revealed that the spent FCC catalyst is predominantly composed of silicon dioxide ($Si_2\ O_3$) at 49.9% and aluminum oxide ($Al_2\ O_3$) at 28.9%. These two oxides constitute nearly 79% of the total composition, indicating a high aluminosilicate content. Other significant components include titanium dioxide (TiO_2) at 7.5%, iron oxide ($Fe_2\ O_3$) at 6%, and lanthanum oxide ($La_2\ O_3$) at 2.4%. The remaining 5.3% is attributed to other minor constituents.

Table 3. Chemical compositions of FCC

Oxides	Content (%)
Si_2O_3	49.9
Al_2O_3	28.9
TiO_2	7.5
Fe_2O_3	6
La_2O_3	2.4
Others	5.3

The XRD pattern of the spent FCC catalyst, presented in Figure 3, exhibits a complex profile characteristic of both amorphous and crystalline phases. A notable feature is the elevated baseline across a wide angular range, particularly evident between 15° and 30° 2θ. This broad hump is indicative of a significant amorphous silica content, suggesting that a large portion of the original zeolite Y structure has degraded into an aluminosilicate glass. This transformation is likely due to exposure to hydrocarbon feedstocks at high temperatures within the FCC unit.

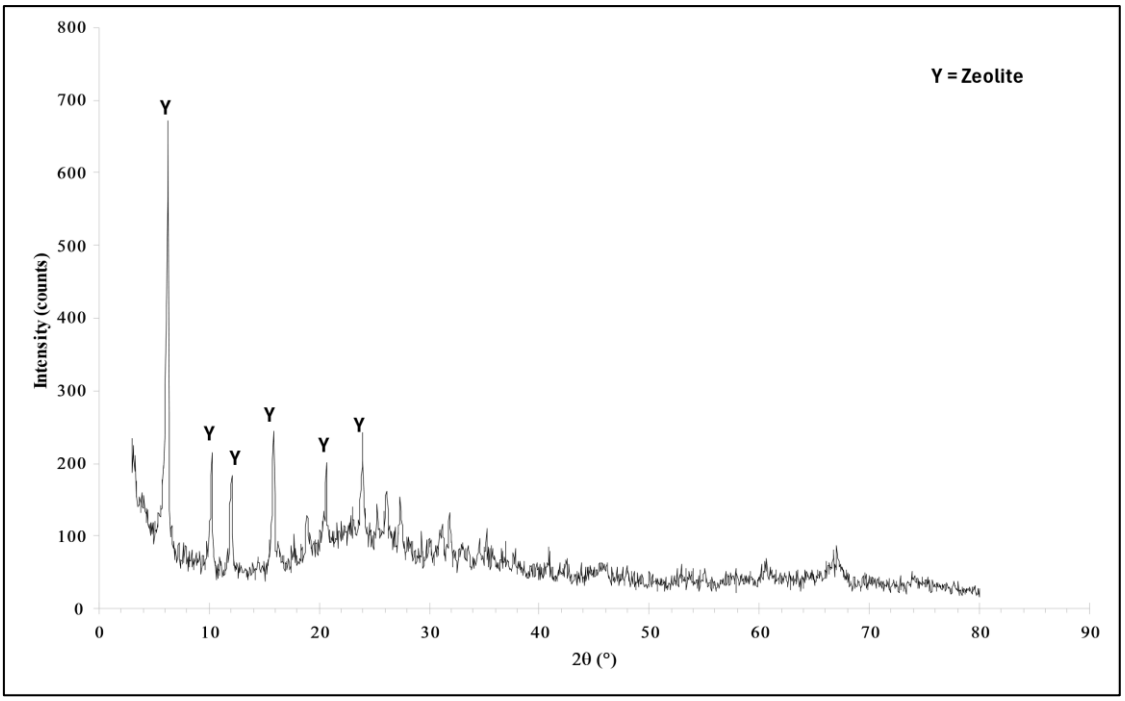

Figure 3. X-Ray data of FCC

Despite the predominantly amorphous nature, the XRD pattern also displays several sharp diffraction peaks, most prominently at low angles (below 10° 2θ) and in the 20-30° 2θ range. These peaks indicate the presence of residual crystalline phases, likely corresponding to zeolitic structures that have not completely broken down under the harsh hydrothermal conditions of the FCC process.

3. Research Methodology

3.1. Experimental Design Overview

The experimental methodology, as shown in Figure 4, encompassed four distinct phases: materials characterization, preliminary testing, mechanical strength assessment, and microstructural analysis. The materials characterization involved XRF and XRD analyses of GGBFS and FCC catalysts to determine their chemical and mineralogical compositions. Mechanical evaluation comprised unconfined compressive strength and splitting tensile strength tests at prescribed curing intervals, while microstructural investigation utilizing SEM and XRD techniques elucidated the fundamental mechanisms governing strength development. This systematic approach enabled a comprehensive assessment of GGBFS-FCC binary blends for sustainable pavement base course applications.

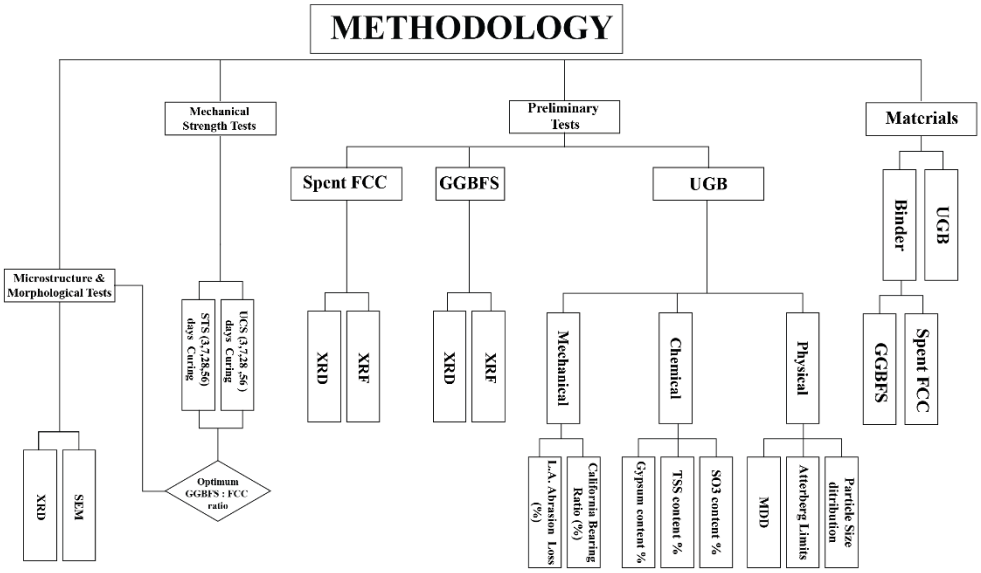

Figure 4. Experimental methodology flowchart

3.2. Mixing proportions

The experimental program involved preparing samples with varying proportions of spent FCC catalyst and GGBFS as a binder for the unbound granular base (UGB) material. The total binder content was fixed at 10% by weight of the dry UGB since this percentage allows clear differentiation of strength variations due to component ratios while minimizing the masking effects that could occur at higher contents where strength differences become less pronounced. The ratio of FCC to GGBFS was varied from 10:90 to 90:10 in increments of 10%. Optimum water content was set at 8% of the total dry weight (UGB + binder) based on the modified Proctor method.

Table 4 provides details on the sample identification and mixing proportions for each experimental combination.

Table 4. Mixing proportions and sample identifications

ID	Binder (%)	FCC: GGBFS	FCC (g)	GGBFS (g)	UGB (g)	Water (g)	Total (g)
M01	10	10:90	35	315	3800	333	4494
M02	10	20:80	70	280	3800	333	4494
M03	10	30:70	105	245	3800	333	4494
M04	10	40:60	140	210	3800	333	4494
M05	10	50:50	175	175	3800	333	4494
M06	10	60:40	210	140	3800	333	4494
M07	10	70:30	245	105	3800	333	4494
M08	10	80:20	280	70	3800	333	4494
M09	10	90:10	315	35	3800	333	4494

3.3. Sample Preparation

The experimental mixtures were prepared using a 30L capacity laboratory mechanical mixer to ensure homogeneous blending of crushed gravel aggregates, ground granulated blast furnace slag (GGBFS), and spent fluid catalytic cracking catalyst (FCC) in predetermined proportions. Water was incorporated during mixing to achieve the specified content for optimal workability. Specimens were compacted in steel cylinder molds (100 mm inner diameter, 200 mm height) in 5 layers, using a vibratory compactor to replicate field densities, targeting a minimum of 95% modified Proctor density. The compaction process was standardized across all samples to ensure consistency. For each mixing proportion, three replicates were prepared to account for statistical variability. Samples were extruded from the molds 24 hours post-compaction and subjected to curing at an ambient room temperature of 25°C. This curing regime was selected to simulate typical in situ conditions for pavement base materials, facilitating gradual pozzolanic reactions while aligning with energy-efficient construction practices.

Testing was conducted at ages 3, 7, 28, and 56 days to evaluate the evolution of material properties over time. This comprehensive approach allows for a thorough assessment of the stabilized base course performance, considering both early-age and long-term characteristics. The sample preparation sequence is presented in Figure 5.

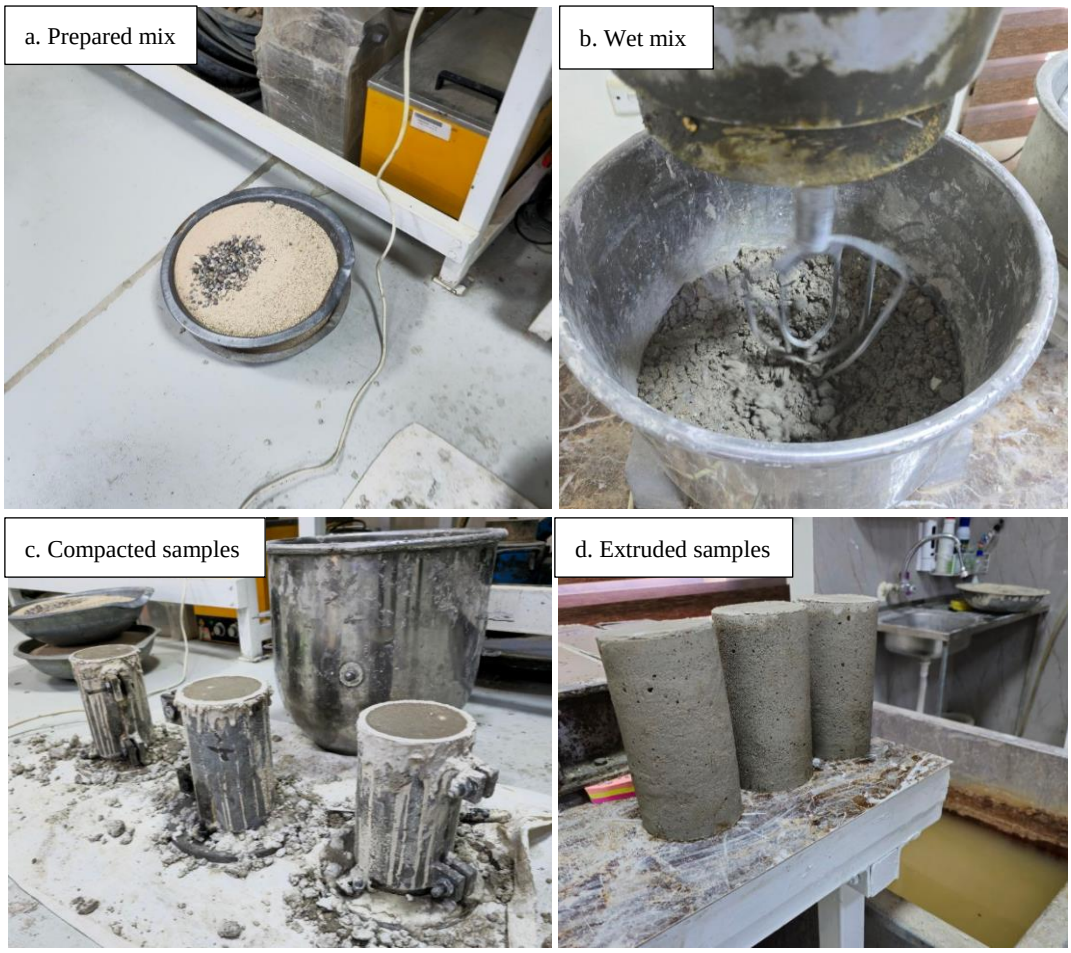

Figure 5. Sample preparation sequence. a: Prepared mix, b: Wet mix, c: Compacted samples, d: Extruded samples

3.4. Testing Program

3.4.1. Unconfined Compressive Strength (UCS)

Unconfined compressive strength (UCS) testing was conducted in accordance with ASTM D1633M-17 [19] to evaluate the mechanical performance of the stabilized base course specimens. The test was performed using a calibrated compression testing machine (Figure 6) with a constant strain rate of 1% per minute. Cylindrical specimens (101 mm diameter, 200 mm height) were trimmed to achieve a length-to-diameter ratio of 2.0 ± 0.1. The prepared specimens were centered on the lower plate of the testing machine. Axial load was applied continuously until failure occurred. The maximum load sustained by the specimen was recorded, and the compressive strength was calculated by dividing the maximum load by the initial cross-sectional area of the specimen. Three replicates were tested for each mixture proportion and curing age to ensure statistical reliability.

Figure 6. Test Apparatus for Unconfined Compressive Strength Test

3.4.2. Splitting Tensile Strength

The splitting tensile strength test for stabilized aggregate base course samples is an important method of determination since it is used in large-scale constructions, such as road construction ASTM C469 [23]. This test consists of placing the cylindrical specimens horizontally and applying a load on them along their vertical diameter until they fail by splitting. Where the tensile strength T is given by:

$$T = \frac{2P}{\pi LD} \quad (1)$$

where P is the maximum load, L is the specimen length, and D is its diameter.

This method provides vital information concerning the bonding between aggregations and tensile behavior of either stabilized or modified aggregates that meet certain strength requirements competent to a particular engineering end use. Test apparatus for the splitting tensile strength test was well shown in Figure 7.

Figure 7. Test Apparatus for Splitting Tensile Strength Test

3.4.2. Scanning Electron Microscope (SEM)

Microstructural analysis of the optimum stabilized base course specimen was conducted using a high-resolution scanning electron microscope (SEM), model INSPECT F50, shown in Figure 8. This field emission SEM enables the examination of sample morphology and elemental composition at nanoscale resolution. The specimen for SEM analysis was prepared by carefully fracturing the sample to expose a fresh, uncontaminated surface. This fragment was mounted on an aluminum stub using conductive carbon tape and sputter-coated with a thin layer of gold to enhance conductivity and image quality. The SEM was operated at an accelerating voltage of 20 kV, with a working distance of approximately 10 mm. Secondary electron imaging was employed to observe topographical features and morphology of hydration products. Energy-dispersive X-ray spectroscopy (EDS) was performed in conjunction with SEM imaging to determine elemental compositions of specific regions and identify hydration products.

Figure 8. INSPECT F50 SEM device

4. Results and Discussion

4.1. Compressive Strength

The unconfined compressive strength (UCS) results for all mix proportions at 3, 7, 28, and 56 days of curing are presented in Figure 9.

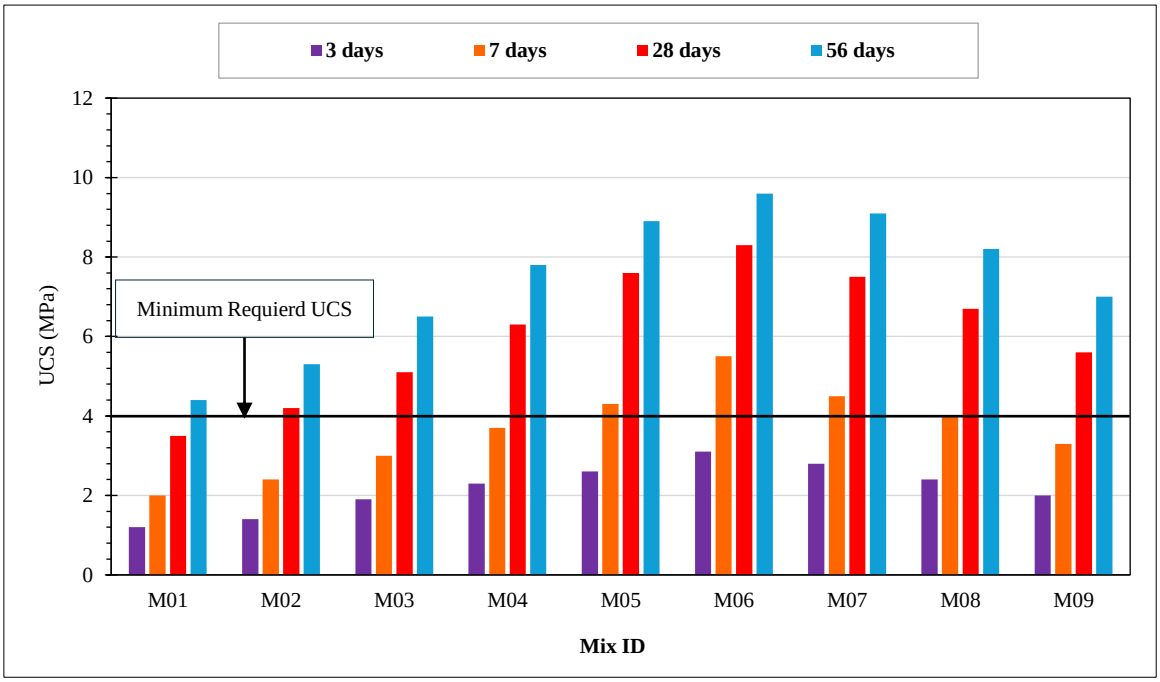

Figure 9. Unconfined compressive strength for different mixes

There is a clear optimal ratio of FCC to GGBFS for maximizing compressive strength. As the FCC content increases from 10% to 60% (M01 to M06), the 56-day strength rises from 4.4 MPa to 9.6 MPa. However, further increases in FCC content beyond 60% (M07 to M09) lead to a decline in strength. This parabolic relationship suggests that the pozzolanic reactivity of FCC contributes positively to strength development up to a certain point, after which the benefits diminish.

This behavior can be explained by the pozzolanic reaction mechanisms. FCC, being rich in reactive silica and alumina, reacts with calcium hydroxide produced by GGBFS hydration to form additional calcium silicate hydrate (C-S-H) gel, which is the primary strength-giving compound in cementitious materials [41]. However, when FCC content exceeds the optimal level, there may be insufficient calcium hydroxide available from GGBFS to fully react with the excess silica, leading to reduced strength gain [42, 43].

The UCS values obtained in this study, particularly the 9.6 MPa achieved by the 60% FCC:40% GGBFS blend at 56 days, demonstrate a significant enhancement in compressive strength. This finding aligns with the results reported by Rasheed et al. (2024) [18], who investigated a composite binder comprising cement bypass dust (CBD) and spent fluid catalytic cracking (FCC) catalyst for sustainable pavement base stabilization. Their study found that a 50:50 CBD/FCC mixture achieved an unconfined compressive strength of 15.6 MPa at 28 days with 10% binder content. The improved UCS in both studies can be attributed to the synergistic cementitious and pozzolanic reactions facilitated by the high calcium content in the binders, leading to the formation of additional calcium silicate hydrate (C-S-H) gel, which densifies the matrix and enhances strength.

The failure patterns of specimens under unconfined compression revealed distinct mechanisms correlating with their measured strength values. The optimal blend (M06) at 56 days exhibited characteristic columnar failure with primary vertical cracks propagating at 10-15° from the loading axis, as shown in Figure 10. This controlled crack propagation pattern, characterized by well-defined vertical fissures and minimal surface spalling, indicates the development of a robust cementitious matrix through effective synergistic interaction between GGBFS and FCC catalyst. The maintained post-failure integrity of these specimens suggests uniform stress distribution and enhanced internal cohesion, consistent with their superior mechanical performance.

Conversely, specimens with lower strength, particularly M01, demonstrated markedly different failure characteristics (Figure 10). These samples exhibited multiple irregular crack patterns with pronounced secondary fissures and peripheral spalling, accompanied by considerable debris accumulation at failure. This less cohesive failure mode suggests incomplete development of the cementitious matrix, attributable to suboptimal binder proportions. The contrast in failure patterns between high- and low-strength specimens provides visual evidence supporting the mechanical property measurements and corroborates the optimal GGBFS-FCC ratio identified through strength testing.

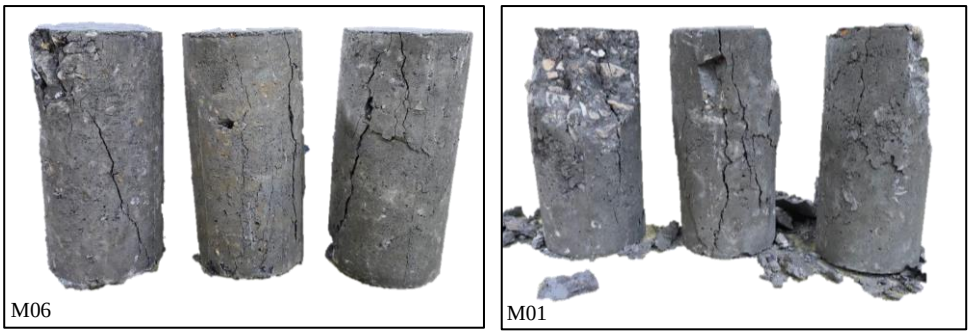

Figure 10. Failure patterns of cylindrical specimens under unconfined compression testing

The rate of strength development also varies with mix composition. All mixes show rapid early strength gain between 3 and 7 days, followed by more gradual increases thereafter. This is consistent with the typical hydration behavior of cementitious systems, where initial reactions occur rapidly before slowing over time [44]. However, mixes with higher FCC content (M05-M07) exhibit more substantial long-term strength gains between 28 and 56 days compared to mixes with lower FCC content. This can be attributed to the slower pozzolanic reactions of FCC compared to the hydraulic reactions of GGBFS [45].

Interestingly, even the lowest performing mix (M01) achieved a 56-day strength of 4.4 MPa, which exceeds the minimum 28-day strength requirement of 4 MPa for cement-treated base materials as specified by many road authorities [46–48]. This suggests that all mix proportions investigated in this study could potentially be suitable for pavement base applications from a strength perspective.

The superior performance of mix M06 (60% FCC:40% GGBFS) can be attributed to an optimal balance between the early strength contribution of GGBFS and the long-term pozzolanic reactions of FCC. GGBFS provides calcium hydroxide for the pozzolanic reaction with FCC while also contributing to early strength gain through its own hydration reactions [45]. Meanwhile, the fine particle size and high surface area of FCC enhance its reactivity, leading to increased formation of C-S-H and C-A-H gel and improved long-term strength [49].

The implications of these results include the feasibility of using larger proportions (up to 100%) of industrial by-products in base materials for pavement application with acceptable strength characteristics. This complementary effect between FCC and GGBFS reflects the potential accomplishment from binary blended systems to enhance the mechanical properties of base courses.

4.2. Splitting Tensile Strength

The splitting tensile strength results for all mixed proportions at 3, 7, 28, and 56 days of curing are presented in Figure 11.

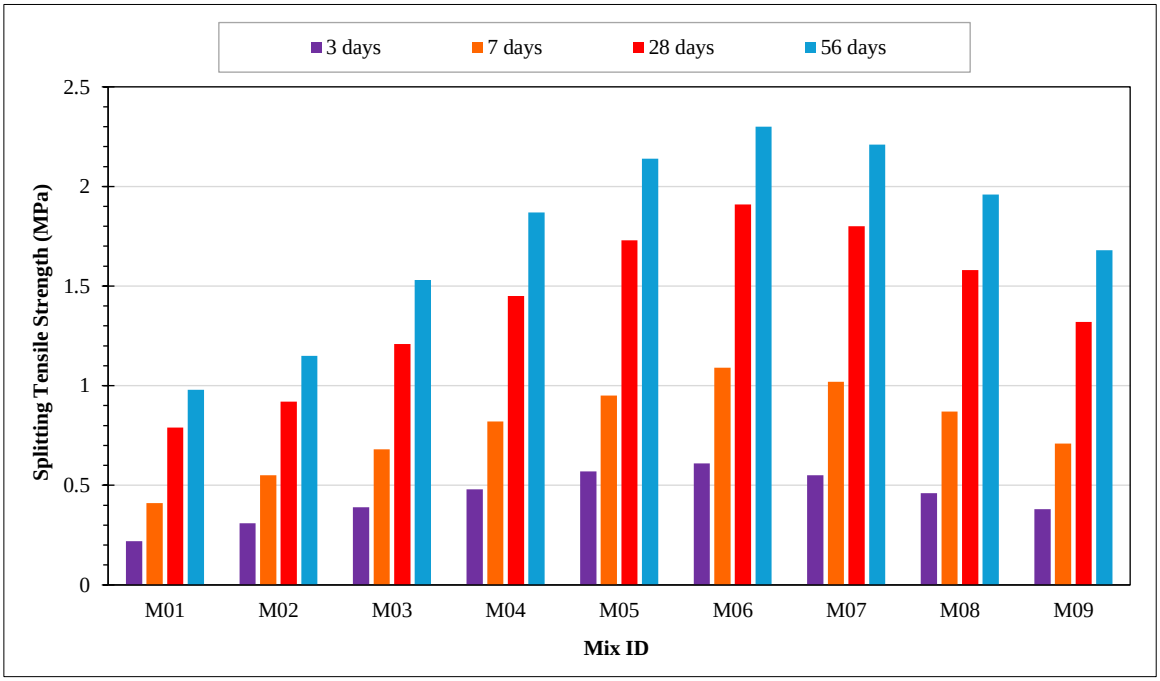

Figure 11. Splitting tensile strength for different mixes

The results show a non-linear relationship between FCC content and tensile strength development. Mix M06 (60% FCC:40% GGBFS) exhibited the highest tensile strength at all ages, reaching 2.30 MPa at 56 days. This optimal blend suggests a synergistic effect between FCC and GGBFS.

Interestingly, the rate of tensile strength gain varies among the mixes. For instance, M05 and M06 show rapid early strength development, while M01 and M02 exhibit more gradual increases. This variability could be attributed to differences in the kinetics of pozzolanic reactions between FCC and the calcium hydroxide produced by GGBFS hydration [50, 51].

The tensile strength values obtained in this study, particularly for mixes M04-M08, are comparable to or exceed those typically reported for conventional cement-treated base materials. For example, Zhao et al. [4] reported 28-day splitting tensile strengths ranging from 0.3 to 1.2 MPa for cement-treated recycled concrete aggregates used in road bases [52].

It's worth noting that the ratio of splitting tensile strength to compressive strength (not shown in this section) for these mixes ranges from 0.18 to 0.24, which is higher than the typical range of 0.08 to 0.14 for conventional concrete [53]. This enhanced tensile-to-compressive strength ratio could be beneficial for pavement applications, potentially improving crack resistance and load distribution capabilities.

The failure mechanisms observed during splitting tensile testing revealed fundamental differences in material response based on binder composition and curing duration. Mix M06 specimens at 56 days curing (Figure 12) exhibited a characteristic single vertical fracture plane that propagated through both the cementitious matrix and aggregate particles. This trans-aggregate fracture pattern, evidenced by the clean splitting surfaces, demonstrates the development of superior interfacial bonding through the optimal GGBFS-FCC interaction. The crack propagation through rather than around aggregate particles indicates that the interfacial transition zone exceeded the inherent strength of the aggregate material.

Mix M01 displayed significantly different fracture characteristics (Figure 12). The failure surfaces showed predominant crack propagation along aggregate-matrix interfaces, with notable matrix deterioration. This interfacial debonding behavior indicates that the aggregate-matrix interface remained the critical failure plane. The observed crack patterns circumnavigating aggregate particles correlate directly with the lower measured tensile strength values and suggest incomplete development of the cementitious matrix.

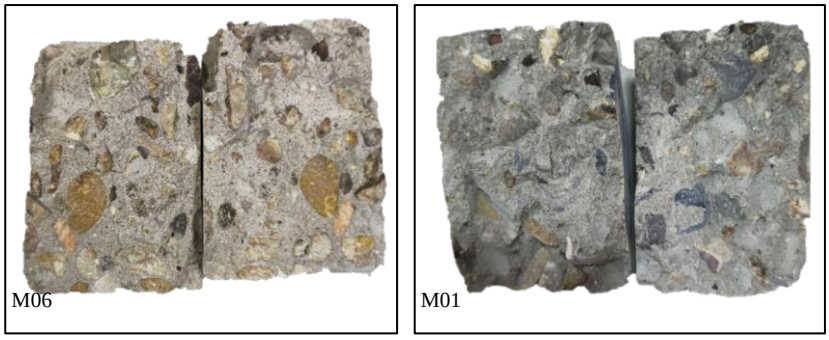

Figure 12. Fracture surface morphology after splitting tensile failure

The long-term strength development observed between 28 and 56 days, particularly for mixes with higher FCC content, indicates ongoing pozzolanic reactions. This continued strength gain could be advantageous in pavement applications, where long-term performance is crucial. However, it also highlights the importance of extended curing periods when using these blends in practice. From a sustainability perspective, the ability to achieve satisfactory tensile strengths using high proportions of industrial by-products aligns with current efforts to reduce the carbon footprint of pavement construction [54].

The splitting tensile strength results observed in this study, with the optimal blend exhibiting a tensile strength of 2.3 MPa at 56 days, are consistent with findings from previous research. Lee & Shin (2019) [55] developed empirical models for predicting the age-dependent development of compressive and split tensile strengths of geopolymer concrete composites with fly ash blended with ground granulated blast furnace slag (GGBFS). Their study indicated that the inclusion of GGBFS contributes to the development of tensile strength over time. The enhancement in tensile strength observed in the present study is likely due to the improved interfacial transition zone and the increased formation of C-S-H gel, which collectively contribute to better stress distribution and crack resistance.

4.3. SEM Observations

Figure 13 presents the scanning electron microscope (SEM) image of mix M06 (60% FCC:40% GGBFS) after 56 days of curing, which was selected as the optimum FCC-GGBFS ratio based on the results of UCS and STS while Figure 14 shows the corresponding X-ray diffraction (XRD) pattern.

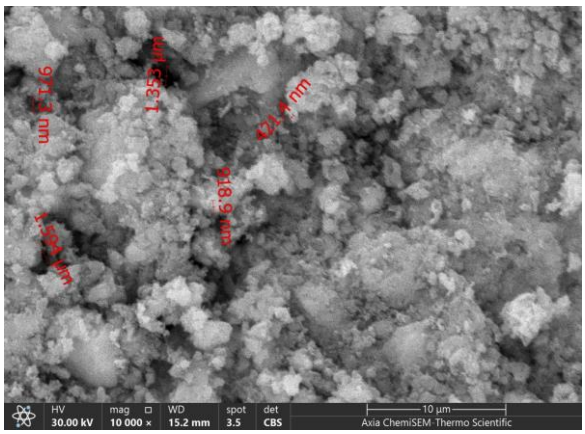

Figure 13. SEM micrograph for the M06 sample

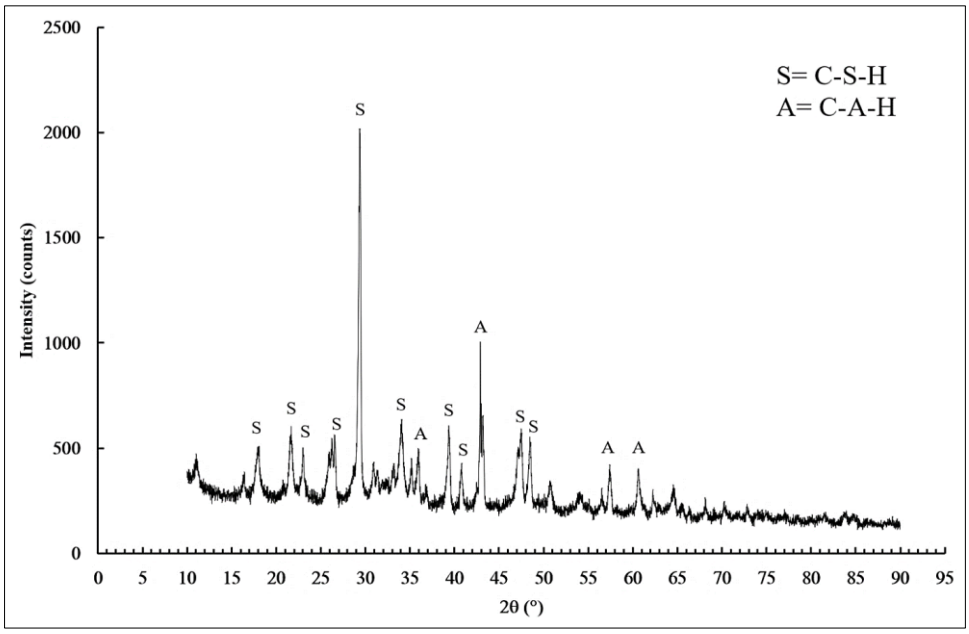

Figure 14. XRD patterns for the M06 sample

The SEM micrograph reveals a dense microstructure with irregularly shaped particles, indicating a distribution of fine to slightly coarser particles. The structure appears compact with some visible pore spaces between particle clusters. This morphology suggests a well-reacted cementitious system with evidence of hydration products forming between larger particles.

The XRD pattern (Figure 14) exhibits multiple crystalline phases present in the M06 sample. The most prominent peak appears at approximately 29-30° 2θ. This peak is typically linked to calcium silicate hydrate (C-S-H) phases, which are crucial in cementitious materials. Alongside this, several other distinct peaks that correspond to calcium aluminate hydrate (C-A-H) are visible throughout the 10-80° 2θ range, indicating a variety of crystalline phases present in the sample [56].

These findings suggest that the M06 sample has undergone significant hydration and chemical reactions, leading to a complex microstructure with multiple crystalline phases. This is in line with a well-developed cementitious system that includes supplementary materials like spent fluid catalytic cracking (FCC) catalyst and ground granulated blast furnace slag (GGBFS).

The microstructural characteristics observed in this study, such as the denser and more homogeneous matrix with evident formation of C-S-H gel, corroborate the mechanical test results and confirm the beneficial effects of GGBFS and FCC catalyst incorporation. This observation is in line with the findings of Amulya & Ravi Shankar [57], who investigated the use of stabilized lateritic and black cotton soils as a base course in flexible pavement. Their study reported that the formation of calcium silicate hydrate and calcium alumino-silicate hydrate structures resulted in a remarkable improvement in the compressive strength, flexure, and fatigue life of treated soils due to dissolved calcium ions from GGBFS reacting with alkali solutions. The microstructural analysis in their study showed closely packed crystal orientation, indicating high strength, which is consistent with the microstructural observations in the present study.

5. Conclusion

This study explored the use of ground granulated blast furnace slag (GGBFS) and spent fluid catalytic cracking (FCC) catalyst as sustainable binders for unbound granular base (UGB) materials. The mechanical and microstructural analyses demonstrated that blending 60% FCC with 40% GGBFS produced the highest performance. The unconfined compressive strength (UCS) peaked at 9.6 MPa after 56 days of curing, surpassing industry standards for base materials. Similarly, the splitting tensile strength reached 2.3 MPa, indicating improved resistance to cracking and mechanical stresses. Microstructural evaluation through SEM and XRD confirmed the formation of dense hydration products, predominantly calcium silicate hydrate (C-S-H) gel, which strengthened the matrix and reduced porosity. These findings affirm the technical feasibility of GGBFS-FCC blends, particularly in applications requiring durable, high-performance base courses. Moreover, the study highlights the synergistic pozzolanic reactions between FCC and GGBFS as a critical factor in achieving these results, underlining the potential for these materials to enhance pavement performance while reducing reliance on conventional cement.

The implications of this research extend beyond mechanical performance, offering a pathway for sustainable construction practices by utilizing industrial by-products and reducing the carbon footprint of pavement materials. The study contributes to the broader goals of circular economy and resource efficiency, addressing both environmental and engineering challenges. However, the research is limited by its focus on laboratory-scale experiments, which do not account for real-world variables such as traffic loading, environmental conditions, and long-term durability. Additionally, while the optimal proportions of FCC and GGBFS were identified, their performance under dynamic and cyclic loading remains unexplored. Future studies should prioritize field validation to evaluate the durability of these materials under actual service conditions. Advanced modeling and life cycle cost analysis are also necessary to establish the economic feasibility of scaling up this approach. By addressing these aspects, the adoption of GGBFS-FCC blends in sustainable pavement construction can be further accelerated.

6. Declarations

6.1. Author Contributions

Conceptualization, S.E.R., M.Y.F., and W.H.H.; methodology, S.E.R.; software, S.E.R.; validation, S.E.R., M.Y.F., and W.H.H.; formal analysis, S.E.R.; investigation, S.E.R.; resources, S.E.R.; data curation, S.E.R.; writing—original draft preparation, S.E.R.; writing—review and editing, S.E.R.; visualization, S.E.R.; supervision, S.E.R.; project administration, S.E.R.; funding acquisition, W.H.H. All authors have read and agreed to the published version of the manuscript.

6.2. Data Availability Statement

The data presented in this study are available in the article.

6.3. Funding

The authors received no financial support for the research, authorship, and/or publication of this article.

6.4. Conflicts of Interest

The authors declare no conflict of interest.

7. References

[1] Gautam, P. K., Kalla, P., Jethoo, A. S., Agrawal, R., & Singh, H. (2018). Sustainable use of waste in flexible pavement: A review. Construction and Building Materials, 180, 239–253. doi:10.1016/j.conbuildmat.2018.04.067.

[2] Balaguera, A., Carvajal, G. I., Albertí, J., & Fullana-i-Palmer, P. (2018). Life cycle assessment of road construction alternative materials: A literature review. Resources, Conservation and Recycling, 132, 37–48. doi:10.1016/j.resconrec.2018.01.003.

[3] Plati, C. (2019). Sustainability factors in pavement materials, design, and preservation strategies: A literature review. Construction and Building Materials, 211, 539–555. doi:10.1016/j.conbuildmat.2019.03.242.

[4] Zhao, Z., Xiao, F., & Amirkhanian, S. (2020). Recent applications of waste solid materials in pavement engineering. Waste Management, 108, 78–105. doi:10.1016/j.wasman.2020.04.024.

[5] Moins, B., France, C., Van den bergh, W., & Audenaert, A. (2020). Implementing life cycle cost analysis in road engineering: A critical review on methodological framework choices. Renewable and Sustainable Energy Reviews, 133. doi:10.1016/j.rser.2020.110284.

[6] Ramírez-Vargas, J. R., Zamora-Castro, S. A., Herrera-May, A. L., Sandoval-Herazo, L. C., Salgado-Estrada, R., & Diaz-Vega, M. E. (2024). A Review of Sustainable Pavement Aggregates. Applied Sciences (Switzerland), 14(16), 7113. doi:10.3390/app14167113.

[7] Sathvik, S., Shakor, P., Hasan, S., Awuzie, B. O., Singh, A. K., Rauniyar, A., & Karakouzian, M. (2023). Evaluating the potential of geopolymer concrete as a sustainable alternative for thin white-topping pavement. Frontiers in Materials, 10. doi:10.3389/fmats.2023.1181474.

[8] Ullas, S., & Bindu, C. S. (2024). Enhancing sustainability in stabilised macadam layer: utilising locally available materials for eco-friendly drainage layers. Innovative Infrastructure Solutions, 9(9), 362. doi:10.1007/s41062-024-01682-4.

[9] ASTM C989/C989M-18a. (2022). Standard Specification for Slag Cement for Use in Concrete and Mortars. ASTM International, Pennsylvania, United States. doi:10.1520/C0989_C0989M-18A.

[10] Gholampour, A., & Ozbakkaloglu, T. (2017). Performance of sustainable concretes containing very high volume Class-F fly ash and ground granulated blast furnace slag. Journal of Cleaner Production, 162, 1407–1417. doi:10.1016/j.jclepro.2017.06.087.

[11] Ika Putra, A., & Shahin, M. A. (2019). Use of slag (with cement) for improving the performance of expansive soil of road pavement subgrade. MATEC Web of Conferences, 276, 05002. doi:10.1051/matecconf/201927605002.

[12] Amulya, S., & Ravi Shankar, A. U. (2020). Replacement of Conventional Base Course with Stabilized Lateritic Soil Using Ground Granulated Blast Furnace Slag and Alkali Solution in the Flexible Pavement Construction. Indian Geotechnical Journal, 50(2), 276–288. doi:10.1007/s40098-020-00426-2.

[13] Arulrajah, A., Mohammadinia, A., Phummiphan, I., Horpibulsuk, S., & Samingthong, W. (2016). Stabilization of Recycled Demolition Aggregates by Geopolymers comprising Calcium Carbide Residue, Fly Ash and Slag precursors. Construction and Building Materials, 114, 864–873. doi:10.1016/j.conbuildmat.2016.03.150.

[14] Ferella, F., Innocenzi, V., & Maggiore, F. (2016). Oil refining spent catalysts: A review of possible recycling technologies. Resources, Conservation and Recycling, 108, 10–20. doi:10.1016/j.resconrec.2016.01.010.

[15] Rodríguez, E. D., Bernal, S. A., Provis, J. L., Gehman, J. D., Monzó, J. M., Payá, J., & Borrachero, M. V. (2013). Geopolymers based on spent catalyst residue from a fluid catalytic cracking (FCC) process. Fuel, 109, 493–502. doi:10.1016/j.fuel.2013.02.053.

[16] Payá, J., Monzó, J., & Borrachero, M. V. (1999). Fluid catalytic cracking catalyst residue (FC3R): An excellent mineral by-product for improving early-strength development of cement mixtures. Cement and Concrete Research, 29(11), 1773–1779. doi:10.1016/S0008-8846(99)00164-7.

[17] Xue, Y., Wei, X., Zhao, H., Wang, T., & Xiao, Y. (2020). Interaction of spent FCC catalyst and asphalt binder: Rheological properties, emission of VOCs and immobilization of metals. Journal of Cleaner Production, 259. doi:10.1016/j.jclepro.2020.120830.

[18] Rasheed, S. E., Fattah, M. Y., Hassan, W. H., & Hafez, M. (2024). Strength and Durability Characteristics of Sustainable Pavement Base Course Stabilized with Cement Bypass Dust and Spent Fluid Catalytic Cracking Catalyst. Infrastructures, 9(12), 217. doi:10.3390/infrastructures9120217.

[19] ASTM D1633-17. (2017). Standard Test Methods for Compressive Strength of Molded Soil-Cement Cylinders. ASTM International, Pennsylvania, United States. doi:10.1520/D1633-17.

[20] Lim, S., & Zollinger, D. G. (2003). Estimation of the Compressive Strength and Modulus of Elasticity of Cement-Treated Aggregate Base Materials. Transportation Research Record, 1837, 30–38. doi:10.3141/1837-04.

[21] Al-Hdabi, A., Al Nageim, H., & Seton, L. (2014). Performance of gap graded cold asphalt containing cement treated filler. Construction and Building Materials, 69, 362–369. doi:10.1016/j.conbuildmat.2014.07.081.

[22] Taha, R. (2003). Evaluation of Cement Kiln Dust-Stabilized Reclaimed Asphalt Pavement Aggregate Systems in Road Bases. Transportation Research Record, II(1819), 11–17. doi:10.3141/1819b-02.

[23] ASTM C469-02e1. (2001). Standard Test Method for Static Modulus of Elasticity and Poisson's Ratio of Concrete in Compression. ASTM International, Pennsylvania, United States. doi:10.1520/C0469-02E01.

[24] Chen, J. J., Thomas, J. J., Taylor, H. F. W., & Jennings, H. M. (2004). Solubility and structure of calcium silicate hydrate. Cement and Concrete Research, 34(9), 1499–1519. doi:10.1016/j.cemconres.2004.04.034.

[25] Wolter, J. M., Schmeide, K., Huittinen, N., & Stumpf, T. (2019). CM(III) retention by calcium silicate hydrate (C-S-H) gel and secondary alteration phases in carbonate solutions with high ionic strength: A site-selective TRLFS study. Scientific Reports, 9(1), 14255. doi:10.1038/s41598-019-50402-x.

[26] Madadi, A., & Wei, J. (2022). Characterization of Calcium Silicate Hydrate Gels with Different Calcium to Silica Ratios and Polymer Modifications. Gels, 8(2), 75. doi:10.3390/gels8020075.

[27] Fan, M. X., Chen, F. X., Zhang, X. Y., Wang, R. K., & Yu, R. (2023). Effect of Ca/Si ratio on the characteristics of alkali-activated ultra-high performance concrete (A-UHPC): From hydration kinetics to microscopic structure development. Construction and Building Materials, 394. doi:10.1016/j.conbuildmat.2023.132158.

[28] Mohajerani, A., Burnett, L., Smith, J. V., Markovski, S., Rodwell, G., Rahman, M. T., Kurmus, H., Mirzababaei, M., Arulrajah, A., Horpibulsuk, S., & Maghool, F. (2020). Recycling waste rubber tyres in construction materials and associated environmental considerations: A review. Resources, Conservation and Recycling, 155. doi:10.1016/j.resconrec.2020.104679.

[29] Alemshet, D., Fayissa, B., Geremew, A., & Chala, G. (2023). Amelioration Effect of Fly Ash and Powdered Ground Steel Slag for Improving Expansive Subgrade Soil. Journal of Engineering (United Kingdom), 1652373. doi:10.1155/2023/1652373.

[30] Kumar, D., Sharma, A., & Singh, K. (2023). Towards Sustainable Stabilization: Utilizing Waste Material as Binder. IOP Conference Series: Earth and Environmental Science, 1110(1), 012002. doi:10.1088/1755-1315/1110/1/012002.

[31] Kedar, H. N., Aware, R., Repale, G., Pankaj, T., & Sangale, P. (2024). Optimizing industrial waste in road construction: a response surface methodology approach. Journal of Building Pathology and Rehabilitation, 9(1), 59. doi:10.1007/s41024-024-00419-1.

[32] Qiu, K., Zeng, G., Shu, B., & Luo, D. (2023). Study on the Performance and Solidification Mechanism of Multi-Source Solid-Waste-Based Soft Soil Solidification Materials. Materials, 16(13), 4517. doi:10.3390/ma16134517.

[33] Zhang, J., Li, C., Ding, L., & Li, J. (2021). Performance evaluation of cement stabilized recycled mixture with recycled concrete aggregate and crushed brick. Construction and Building Materials, 296. doi:10.1016/j.conbuildmat.2021.123596.

[34] Ministry of Housing and Construction. (2003). Iraqi Standard Specifications for Roads and Bridges. Ministry of Housing and Construction: Baghdad, Iraq.

[35] ASTM C1580-09. (2010). Standard Test Method for Water-Soluble Sulfate in Soil. ASTM International, Pennsylvania, United States. doi:10.1520/C1580-09.

[36] ASTM D 2974-87. (1993). Standard Test Methods for Determining the Water (Moisture) Content, Ash Content, and Organic Material of Peat and Other Organic Soils. ASTM International, Pennsylvania, United States.

[37] ASTM D4318-10. (2014). Standard Test Methods for Liquid Limit, Plastic Limit, and Plasticity Index of Soils. ASTM International, Pennsylvania, United States. doi:10.1520/D4318-10.

[38] ASTM C131/C131M-20. (2020). Standard Test Method for Resistance to Degradation of Small-Size Coarse Aggregate by Abrasion and Impact in the Los Angeles Machine. ASTM International, Pennsylvania, United States. doi:10.1520/C0131_C0131M-20.

[39] ASTM C131/C131M-14. (2014). Standard Test Method for Resistance to Degradation of Small-Size Coarse Aggregate by Abrasion and Impact in the Los Angeles Machine. ASTM International, Pennsylvania, United States. doi:10.1520/C0131_C0131M-14.

[40] ASTM D1557-12(2021). (2021). Standard Test Methods for Laboratory Compaction Characteristics of Soil Using Modified Effort (56,000 ft-lbf/ft^3 (2,700 kN-m/m^3)). ASTM International, Pennsylvania, United States. doi:10.1520/D1557-12R21.

[41] Torres Agredo, J., BAQUERO, E. A., & Silva, A. R. (2009). Evaluation of the pozzolanic activity of fluid catalytic cracking residue. Dyna, 76(158), 49-53.

[42] Venkatakrishanaiah, R. (2013). Experimental Study on Strength of High-Volume High Calcium Fly Ash Concrete. IOSR Journal of Mechanical and Civil Engineering, 5(4), 48–54. doi:10.9790/1684-0544854.

[43] Padmanabhan, R., Bhandari, A., Verghese, J. P., Jain, A. N., Rai, T. D., Rooby, J., & T, S. (2020). Mechanical Properties of High Calcium Flyash- GGBFS Geopolymer Paste, Mortar and the Effect of Glass Fibre Mesh on the Strength of Geopolymer Mortar Tile. International Journal of Innovative Technology and Exploring Engineering, 9(6), 722–729.

[44] Mohamed, O. A. (2019). Effect of mix constituents and curing conditions on compressive strength of sustainable self-consolidating concrete. Sustainability (Switzerland), 11(7), 2094. doi:10.3390/su11072094.

[45] Ahmed, A. (2019). Chemical Reactions in Pozzolanic Concrete. Modern Approaches on Material Science, 1(4), 128-133. doi:10.32474/mams.2019.01.000120.

[46] Sharma, A. (2019). Durability and Strength Analysis of Cement Treated Soils for Sub-Base and Base Layers of Pavement. International Journal for Research in Applied Science and Engineering Technology, 7(9), 50–57. doi:10.22214/ijraset.2019.9008.

[47] Otieno, M. O., Kabubo, C., & Gariy, Z. A. (2023). A Comparative Investigation on Cement Stabilized Lateritic Soil Admixed with Sugarcane Bagasse Ash and Saw Dust Ash for use in Road Base. International Journal of Engineering Trends and Technology, 71(5), 115–124. doi:10.14445/22315381/IJETT-V71I5P211.

[48] KC, N., Aryal, R., Joshi, B. R., & Shahi, P. B. (2023). Strength of Cement Treated Base Courses in the Flexible Pavement Design for Pathlaiya- Nijgadh Section of East-West Highway of Nepal. Himalayan Journal of Applied Science and Engineering, 4(1), 52–61. doi:10.3126/hijase.v4i1.56870.

[49] Elyasigorji, F., Farajiani, F., Hajipour Manjili, M., Lin, Q., Elyasigorji, S., Farhangi, V., & Tabatabai, H. (2023). Comprehensive Review of Direct and Indirect Pozzolanic Reactivity Testing Methods. Buildings, 13(11), 2789. doi:10.3390/buildings13112789.

[50] Sandybay, S., Shon, C. S., Tukaziban, A., Syzdykov, D., Orynbassarov, I., Zhang, D., & Kim, J. R. (2022). Blended Basic Oxygen Furnace (BOF) Slag with Ground Granulated Blast Furnace Slag (GGBFS) as a Pozzolanic Material. Materials Science Forum, 1053 MSF, 331–337. doi:10.4028/p-q7n2cu.

[51] Jeong, J.-Y., Jang, S.-Y., Choi, Y.-C., Jung, S.-H., & Kim, S.-I. (2015). Effects of Replacement Ratio and Fineness of GGBFS on the Hydration and Pozzolanic Reaction of High-Strength High-Volume GGBFS Blended Cement Pastes. Journal of the Korea Concrete Institute, 27(2), 115–125. doi:10.4334/jkci.2015.27.2.115.

[52] Gao, M., Dai, J., Jing, H., Ye, W., & Sesay, T. (2023). Investigation of the performance of cement-stabilized magnesium slag as a road base material. Construction and Building Materials, 403. doi:10.1016/j.conbuildmat.2023.133065.

[53] Mehta, P.K. and Monteiro, P.J.M. (2006) Concrete: Microstructure, Properties, and Materials (3rd Ed.). McGraw-Hill, New York, United States.

[54] Shi, X., Mukhopadhyay, A., Zollinger, D., & Grasley, Z. (2019). Economic input-output life cycle assessment of concrete pavement containing recycled concrete aggregate. Journal of Cleaner Production, 225, 414–425. doi:10.1016/j.jclepro.2019.03.288.

[55] Lee, S., & Shin, S. (2019). Prediction on compressive and split tensile strengths of GGBFS/FA based GPC. Materials, 12(24), 4198. doi:10.3390/MA12244198.

[56] Silva, L. A., Nahime, B. O., Lima, E. C., Akasaki, J. L., & Reis, I. C. (2020). XRD investigation of cement pastes incorporating concrete floor polishing waste. Ceramica, 66(380), 373–378. doi:10.1590/0366-69132020663802956.

[57] Amulya, S., & Ravi Shankar, A. U. (2020). Use of Stabilized Lateritic and Black Cotton Soils as a Base Course Replacing Conventional Granular Layer in Flexible Pavement. International Journal of Geosynthetics and Ground Engineering, 6(1), 5. doi:10.1007/s40891-020-0184-8.